Whispering-Gallery Modes and Permeability Tensor Measurements in Magnetized Ferrite Resonators

Jerzy Krupka, Pierre Blondy, Dominique Cros, Pierre Guillon, *Senior Member, IEEE,* and Richard G. Geyer

***Abstract*—Whispering-gallery modes in axially magnetized ferrite disk samples have been studied using rigorous Rayleigh–Ritz and finite-element analyses. The influence of radial magnetization on the resonant frequencies of both WGE and WGH modes was investigated, both theoretically and experimentally. Permeability tensor components of biased ferrites were determined from measurements of the resonant frequencies of the WGH_{n00} and the WGE_{n00} mode families.**

I. Introduction

A NUMBER OF papers have recently been published on whispering-gallery modes in dielectric resonators and their applications [1]–[8]. These modes are of particular interest at millimeter-wave frequencies and for extremely high-Q device applications [7], [8] since conductor losses are negligible for resonators operating at high azimuthal mode numbers. This paper gives a resonant frequency analysis of biased ferrite resonators using both the Rayleigh–Ritz [9] and finite-element method (FEM). In particular, whispering-gallery modes in magnetized ferrite resonators are studied. The results demonstrate that all permeability tensor components of microwave ferrites can be derived from measurements of identified whispering-gallery-mode resonant frequencies versus static magnetic field bias of the ferrite disk resonator under test.

II. Theory

The model of the resonator under analysis for a uniform axial static magnetic field bias is illustrated in Fig. 1. The dimensions and permittivity of the resonant structure used in experiments are also shown in Fig. 1. Rayleigh–Ritz [9] and finite-element [10] analyses are used for computations of the resonant frequencies. In the Rayleigh–Ritz method, 125 rotational and 80 potential basis functions of an empty cavity were used, whereas in finite-element analysis, a mesh with 351 elements was employed. Nedelec's second-order polynomial interpolation [11] was applied to represent the H_r and H_z magnetic field components on the same geometrical element; Lagrange's second-order polynomial was employed to represent the rH_ϕ component. These dual polynomial interpolation representations of the field components do not generate spurious (nonphysical) solutions that can otherwise occur with pure Lagrangian polynomial elements.

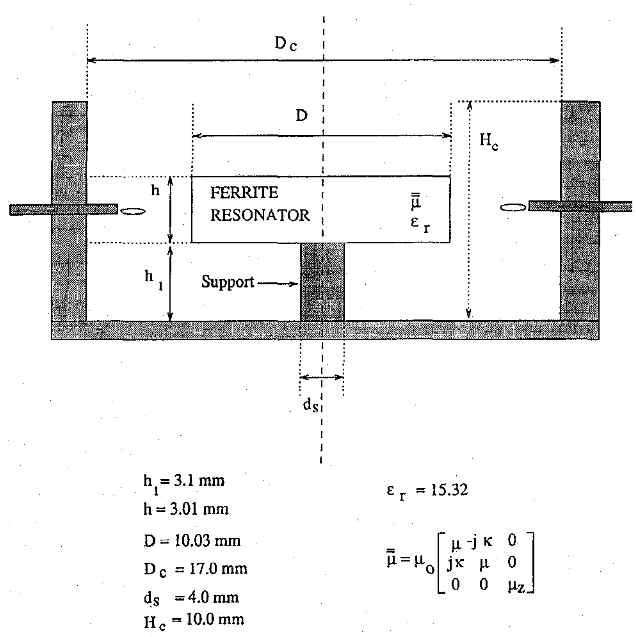

Fig. 1. Schematic diagram of resonant structure under analysis. Perfect conductor wall is assumed at the top of the structure for computations. Dimensions shown correspond to dimensions of structure used in experiments.

The static magnetic field interior to a ferrite disk situated axially in an external magnetic field is not spatially uniform, especially in the region close to its lateral surface. This nonuniformity arises from demagnetization effects. Demagnetization is important and should not be neglected unless the ferrite is saturated. The mesh for finite-element analysis that takes demagnetization into account is given in Fig. 2. The ferrite resonator is subdivided into two regions in which the radial static field components are oppositely directed, while the axial static field components are in the same direction. A radial static field leads to two additional off-diagonal components in the permeability tensor:

$$\bar{\bar{\mu}}_u = \mu_0 \begin{bmatrix} \mu & -j\kappa & 0 \\ j\kappa & \mu_\phi & -j\eta \\ 0 & j\eta & \mu_z \end{bmatrix},$$

$$\bar{\bar{\mu}}_l = \mu_0 \begin{bmatrix} \mu & -j\kappa & 0 \\ j\kappa & \mu_\phi & j\eta \\ 0 & -j\eta & \mu_z \end{bmatrix}. \quad (1)$$

These have opposite signs in the upper ($\bar{\bar{\mu}}_u$) and lower ($\bar{\bar{\mu}}_l$) subregions.

Manuscript received October 17, 1995; revised March 20, 1996.

J. Krupka is with the Instytut Mikroelektroniki i Optoelektroniki, Politechnika Warszawska, Koszykowa 75, Poland.
P. Blondy, D. Cros, and P. Guillon are with IRCOM, U.R.A. CNRS 356, Universite de Limoges, Faculté des Sciences, 87060 Limoges Cedex, France.
R. G. Geyer is with the Electromagnetic Fields Division, National Institute of Standards and Technology, Boulder, CO 80303 USA.

Publisher Item Identifier S 0018-9480(96)04712-6.

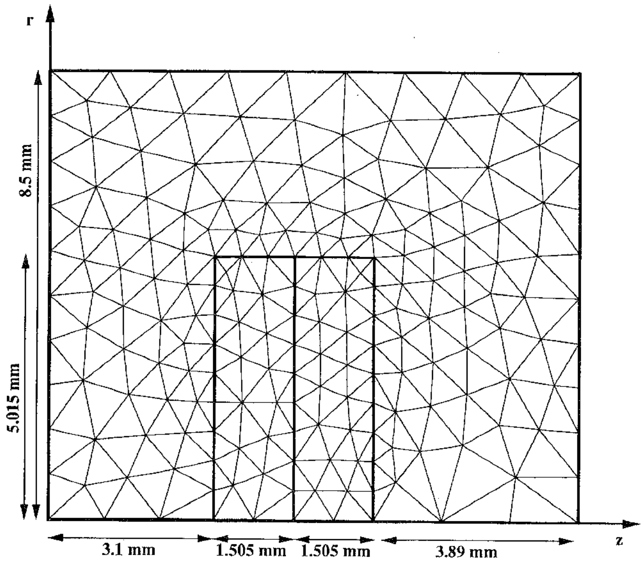

Fig. 2. Finite-element analysis mesh for analysis of resonant structure with radial magnetization.

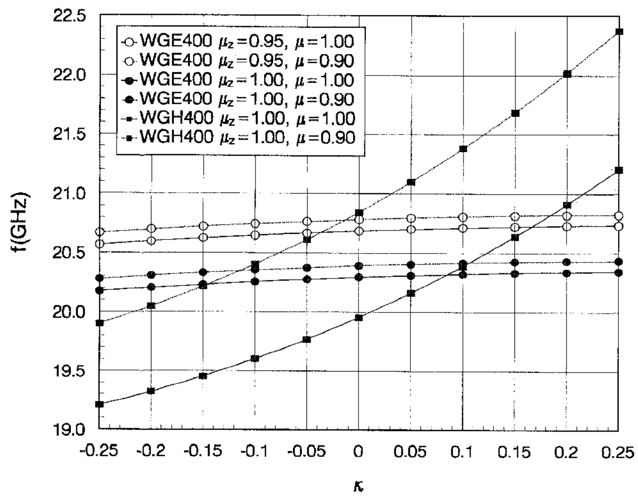

Fig. 3. Theoretical dependence of WGH_{400} and WGE_{400} mode resonant frequencies on permeability tensor components for axially magnetized ferrite disk having parameters given in Fig. 1. WGH_{400} mode family curves for $\mu_z = 0.95$ and $\mu_z = 1.00$ overlie each other with scale of this figure. Dimensions of the resonant structure are given in Fig. 1.

III. Whispering-Gallery Modes in a Magnetized Disk

Computed values of resonant frequencies for the WGH_{400} and WGE_{400} modes are given in Fig. 3 for various assumed values of the permeability tensor components in a magnetized disk. These calculations were obtained with the Rayleigh–Ritz method. A uniform longitudinal (axial) bias was also assumed. The κ and μ components have much greater influence on the resonant frequencies of the WGH mode family than on those of the WGE mode family. The magnetic field for WGH modes is similar to TM modes. On the other hand, the μ_z component significantly affects resonant frequencies of the WGE mode family. Because the WGH mode family resonance curves for $\mu_z = 0.95$ and $\mu_z = 1$ differ by only a few megahertz, they are not presented here. The same results apply for higher-order azimuthal mode numbers. WGH_{400} mode magnetic field distributions are evaluated using finite-element analysis for three cases: $\kappa = 0$, $\kappa = -0.25$, and $\kappa = +0.25$. These three cases are illustrated in Figs. 4–6 and correspond to a demagnetized ferrite disk resonator and a magnetized ferrite disk resonator with two (right and left) circular polarizations of the rf field. Significant differences in the magnetic field distributions between these cases are observed. Similar computations of the magnetic field distribution were performed for the WGH_{400} modes, but exhibited only small differences and are not given here.

Resonant frequency computational results for the WGH_{400} and WGE_{400} modes are summarized in Table I for various values of the off-diagonal components of the permeability tensor in the presence of an additional radial bias. If the static magnetic field bias is axially directed, the average radial magnetization in the upper and lower parts of the ferrite disk resonator (whose static permeability is greater than one) is oppositely directed in the radial coordinate. This corresponds to the resonant frequencies marked with asterisks in Table I. The resonant frequency split due to radial magnetization is about five times smaller for the WGH_{400} modes than for the WGE_{400} modes. On the other hand, the resonant frequency split due to axial magnetization is about 20 times larger for the WGH_{400} modes than for the WGE_{400} modes.

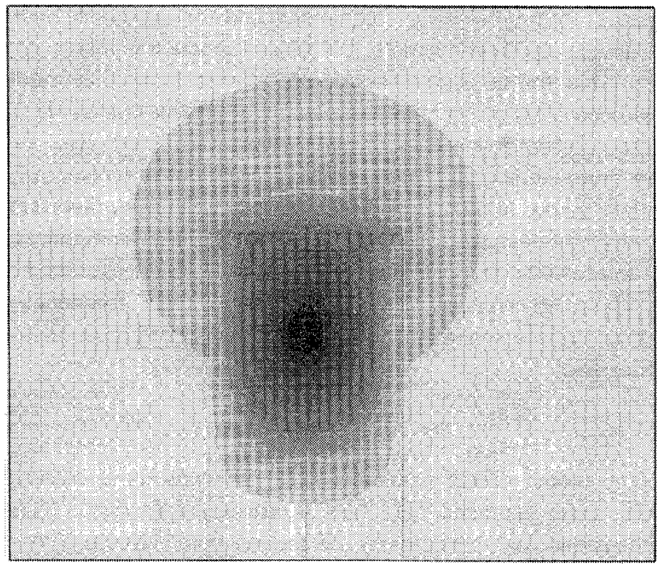

Fig. 4. Distribution of the magnetic field (modulus of $\vec{H}$) computed using finite element analysis for the WGH_{400} mode of ferrite resonator with $\kappa = 0$, $\mu = 1$, and $\mu_z = 1$. Mesh division of structure is given in Fig. 2.

IV. Permeability Tensor Component Measurements

Both cavity and dielectric ring resonator techniques have been used for permeabilty tensor measurements at frequencies less than 10 GHz [12]–[15]. Although these techniques may be employed for permeability tensor measurements at higher frequencies, accuracy suffers. There are several reasons for this decrease in measurement accuracy. Firstly, the Q-factor for metal cavities and dielectric resonators becomes lower with increasing frequency. Secondly, the sample dimensions become smaller with increasing frequency. Therefore, the use

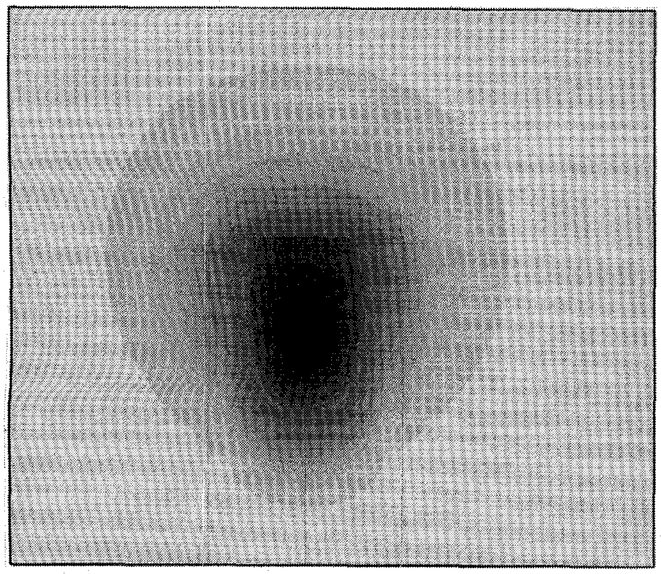

Fig. 5. Distribution of the magnetic field (modulus of $\vec{H}$) computed using finite element analysis for the WGH_{400} mode of ferrite resonator with $\kappa = -0.25$, $\mu = 1$, and $\mu_z = 1$. Mesh division of structure is given in Fig. 2.

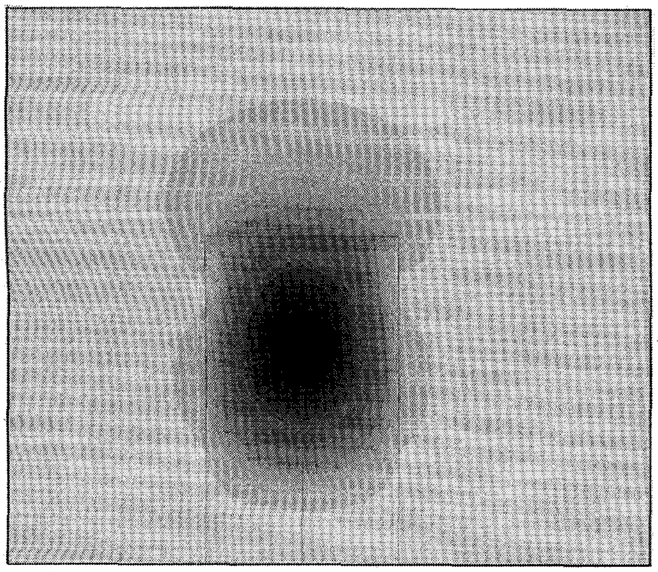

Fig. 6. Distribution of the magnetic field (modulus of $\vec{H}$) computed for the WGH_{400} mode of ferrite resonator with $\kappa = +0.25$, $\mu = 1$, and $\mu_z = 1$. Mesh division of structure is given in Fig. 2.

of whispering gallery modes for permeability tensor measurements at frequencies greater than 10 GHz becomes quite attractive since their Q-factors depend principally on the intrinsic ferrite material losses. The ferrite sample dimensions also remain reasonably large, even for frequencies up to 100 GHz.

In this paper we propose that permeability tensor components of longitudinally magnetized ferrites be determined from measurements of WGH_{n00} and WGE_{n00} resonant frequencies as a function of static magnetic field bias on circular disk samples. A polycrystalline yttrium iron garnet (YIG) ferrite sample, having a saturation magnetization M_s = 140 kA/m,

TABLE I
WGH_{400} AND WGE_{400} MODE RESONANT FREQUENCIES VERSUS OFF-DIAGONAL COMPONENTS OF PERMEABILITY TENSOR FOR NONUNIFORM BIAS. ($\mu = \mu_\phi = \mu_z = 1.0$. REMAINING PARAMETERS OF RESONANT STRUCTURE ARE THE SAME AS IN FIG. 1)

κ	η	f (GHz) WGH_{400}	f (GHz) WGE_{400}
0.00	0.00	19.887	20.350
0.00	−0.10	19.896	19.970
0.00	+0.10	19.888	20.757
−0.25	0.00	19.110	20.247
−0.25	−0.10	19.127*	19.868*
−0.25	+0.10	19.106	20.651
+0.25	0.00	21.161	20.384
+0.25	−0.10	21.091	20.014
+0.25	+0.10	21.239*	20.780*

was used in the experiments reported here. The dimensions and permittivity of the ferrite resonator are given in Fig. 1. The sample was biased in the air gap of a large electromagnet and rf-excited with adjustable coupling loops connected to an automatic network analyzer. Measurement results are shown in Figs. 7–9. The behavior of the WGH_{n00} resonant frequencies is very similar to resonant frequencies of lower-order modes in a cavity or dielectric ring resonator partially filled with a magnetized ferrite sample [14], [16]. A large split between WGE_{n00} resonant frequencies is observed that corresponds to modes polarized in opposite directions in a partially magnetized sample. Typically, a sample is only partially magnetized when the external static magnetic induction field is 0.05–0.3 T. Table I shows that this phenomenon is due to nonuniform static magnetization of the sample in the vicinity of its lateral surface. For large external magnetic field biases (above 0.4 T), the sample is saturated and the behavior of WGE_{n00} resonant frequencies is the same as that expected for a sample that has a *uniform* longitudinal bias. Comparison of measured right- and left-circularly polarized WGE_{400} resonant frequency splitting for a partially saturated sample with the computational results given in Table I demonstrates that the frequency split due to radial magnetization for the WGH_{400} does not constitute more than 2–3% of the resonant frequency split arising from axial magnetization. Hence, two components of the permeability tensor may be determined from measurements of the resonant frequencies of two oppositely polarized WGH_{n00} modes. The third component μ_z can be ascertained from the average of two WGE_{n00} mode resonant frequencies. Computations of κ and μ are made from rigorous evaluations of WGH_{n00} mode resonant frequencies for a given κ and μ. These evaluations are made by applying the Newton iteration method to the eigenvalue equations

$$\begin{aligned} F_1(\mu, \kappa, f_{WGH+}) &= 0 \\ F_2(\mu, \kappa, f_{WGH-}) &= 0 \end{aligned} \tag{2}$$

where f_{WGH+} and f_{WGH-} are the resonant frequencies corresponding to the two WGH_{n00} modes and F_1 and F_2 are functions whose values are computed using the Rayleigh–Ritz technique for the given resonant structure.

Since computations of F_1 and F_2 are time-consuming, we computed them for only a certain number of κ and μ

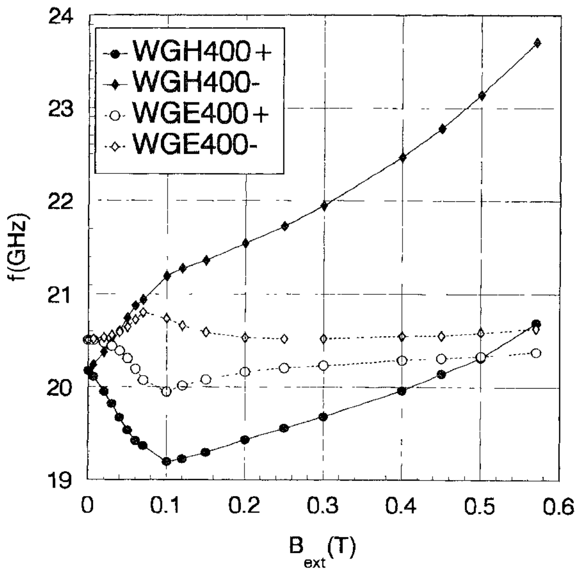

Fig. 7 Measured resonant frequencies of axially magnetized yttrium iron garnet disk versus external static magnetic induction for WGH_{400} and WGE_{400} mode families. Dimensions of resonant structure are given in Fig. 1.

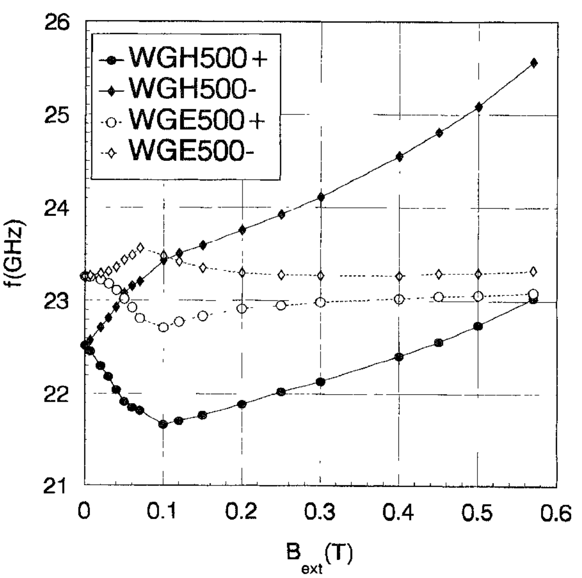

Fig. 8. Measured resonant frequencies of axially magnetized yttrium iron garnet disk versus external static magnetic induction for WGH_{500} and WGE_{500} mode families Dimensions of resonant structure are given in Fig. 1.

values. Two-dimensional second-order polynomial interpolation was then used to evaluate F_1 and F_2 for other values of κ and μ. For each bias, the values of κ and μ were computed as solutions to the system of (2) at a reference frequency. This reference frequency was taken to be the average of the minimum and maximum frequencies of the oppositely polarized WGH_{n00} modes with a fixed azimuthal mode number. The frequency dependence of κ and μ was taken into account in this procedure. For a ferrite above saturation, frequency corrections were made with the well-known Polder relations describing the frequency dependence of κ and μ. For partially saturated ferrites, frequency corrections were made using the expressions given by Green and Sandy [14].

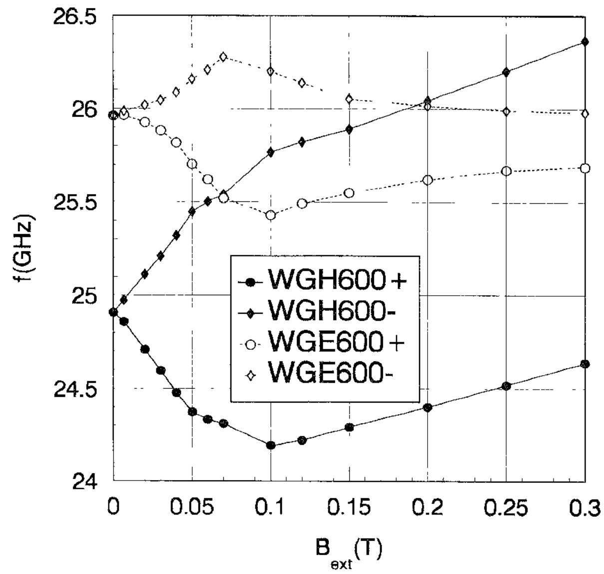

Fig 9 Measured resonant frequencies of axially magnetized yttrium iron garnet disk versus external static magnetic induction for WGH_{600} and WGE_{600} mode families Dimensions of resonant structure are given in Fig. 1.

The resonant frequencies of the WGE modes depend strongly on μ_z (Fig. 3). Once κ and μ are known, μ_z may be determined from

$$F_3(\mu, \kappa, \mu_z, f_{WGE\,av}) = 0 \quad (3)$$

where F_3 is the corresponding eigenvalue equation and where $f_{WGE\,av}$ is the average of the two oppositely polarized WGE_{n00} mode resonant frequencies measured at the same bias for which κ and μ were computed.

Computational results of the magnetic permeability tensor components from the measurement data shown in Figs. 7–9 are given in Figs. 10–12 for different azimuthal mode numbers. Since changes in μ_z are small over the range of applied static field bias, μ_z computations are only presented for the lowest azimuthal mode number, $n = 4$. The dependent of the tensor magnetic permeability components with static field bias is similar to that measured at lower frequencies [12]–[16]. Scalar permeability values corresponding to no static bias agree quite well with values that can be determined from Scholemann's formula [16].

For ferrites under test that have low saturation magnetizations, magnetic losses are too small to be measurable at low bias field levels (far from ferromagntic resonance). The Q-factor of the WGH_{600} mode, with an external bias below 0.3 T applied to the polycrystalline YIG sample, was approximately 4800 at 25 GHz and was essentially constant as a function of magnetization. Since conductor losses can be neglected for whispering-gallery-mode resonators, the dielectric loss tangent of the YIG ferrite was found to be 2.0×10^{-4} at 25 GHz.

V. Summary

Accurate computations of the resonant frequencies of whispering-gallery modes in axially magnetized ferrites

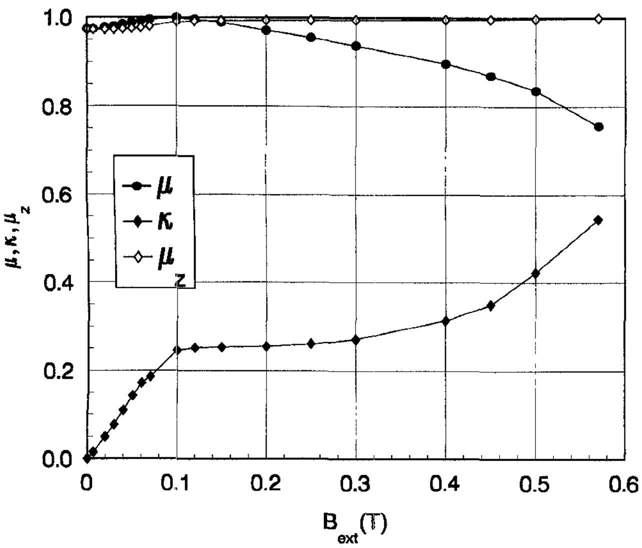

Fig. 10. Permeability tensor components of yttrium iron garnet versus static external magnetic induction at the reference frequency equal to 21.5 GHz. Data computed from measurements of resonant frequencies for WGH_{400} and WGE_{400} mode families.

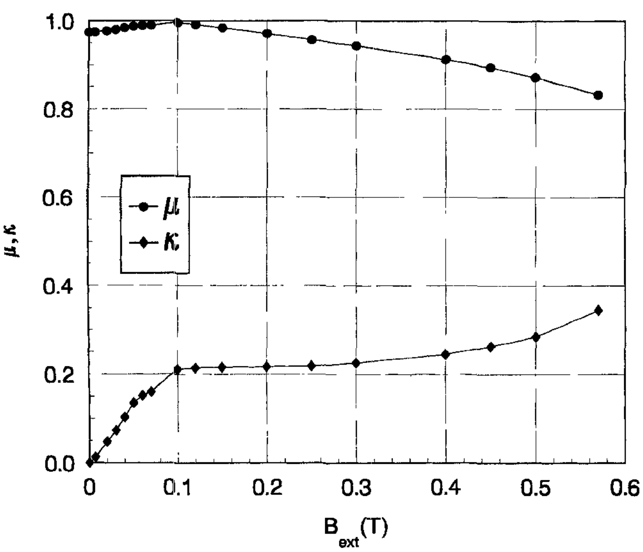

Fig. 11. Permeability tensor components of yttrium iron garnet versus static external magnetic induction at the reference frequency equal to 24.0 GHz. Data computed from measurements of resonant frequencies for WGH_{500} mode family.

may be performed with Rayleigh–Ritz and FEM. Resonant frequency changes due to sample radial magnetization can also be modeled using the FEM.

Whispering gallery modes may be used for the determination of the permeability tensor at frequencies between 20–100 GHz, where the accuracy of cavity and dielectric ring resonator measurements is limited. Measurements at several different frequencies can be performed with the use of a single sample.

Resonant frequencies for the WGE_{n00} modes of a partially magnetized ferrite disk sample placed in an axially directed external magnetic field bias are strongly affected by sample radial magnetization. Radial magnetization arises from a nonuniform static magnetic field distribution near the lateral surface of the ferrite disk. Resonant frequencies of the WGH_{n00} modes, however, remain almost unchanged.

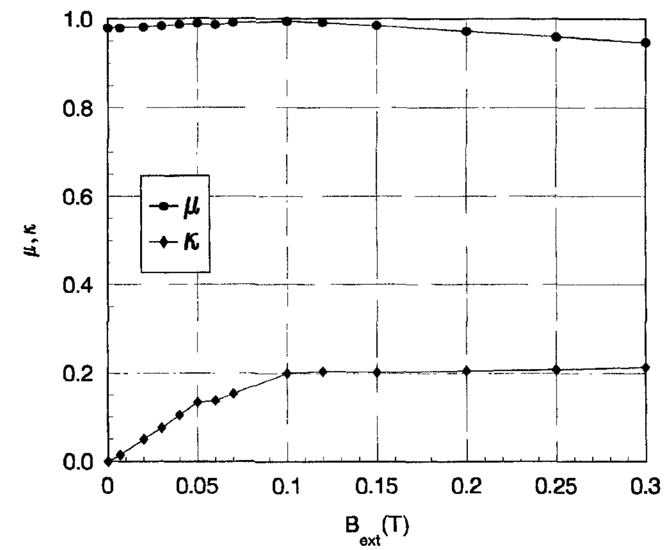

Fig. 12. Permeability tensor components of yttrium iron garnet versus static external magnetic induction at the reference frequency equal to 25.0 GHz. Data computed from measurements of resonant frequencies for WGH_{600} mode family.

REFERENCES

[1] J. R. Wait, "Electromagnetic whispering gallery modes in a dielectric rod," *Radio Sci.*, vol. 2, pp. 1005–1017, 1967.
[2] J. Arnaud, "Note on the use of whispering gallery modes in communications," Bell Lab. memorandum, Sept. 1971.
[3] D. Cros and P. Guillon, "Whispering gallery dielectric resonator modes for W-band devices," *IEEE Trans. Microwave Theory Tech.*, vol. MTT-38, pp. 1667–1674, Nov. 1990.
[4] K. Matsumura, K. Shiraishi, and I. Okada, "Whispering gallery mode resonance in an elliptic dielectric disk for millimeter through optical wave application," in *Proc. 23rd European Microwave Conf.*, Madrid, Spain, Sept. 1993, pp. 608–610.
[5] W. Gross and F. J. Grandorf, "Design of series feedback millimeter oscillator employing whispering gallery mode resonator," in *Proc. 22nd European Microwave Conf.*, Helsinki, Finland, Aug. 1992, pp. 491–496.
[6] J. Krupka, D. Cros, M. Aubourg, and P. Guillon, "Study of whispering gallery modes in anisotropic single crystal dielectric resonators," *IEEE Trans. Microwave Theory Tech.*, vol. 42, pp. 56–61, Jan. 1994.
[7] A. J. Giles, A. G. Mann, S. K. Jones, D. G. Blair, and M. J. Buckingham, "A very high stability sapphire loaded superconducting cavity oscillator," *Physica B*, vol. 165, pp. 145–146, 1990.
[8] M. E. Tobar, A. J. Giles, S. Edwards, and J. H. Searls, "High-Q thermoelectric-stabilized sapphire microwave resonators for low-noise applications," *IEEE Trans. Ultrason., Ferroelect., Freq. Contr.*, vol. 41, pp. 391–395, May 1994.
[9] J. Krupka, "Resonant modes in shielded cylindrical ferrite and single crystal dielectric resonators," *IEEE Trans. Microwave Theory Tech.*, vol. 37, pp. 691–697, Apr. 1989.
[10] M. Aubourg and P. Guillon, "A mixed finite element formulation for microwave device probles: Application to MIS structure," *J. Electromagn. Waves Appl.*, vol. 5, no. 415, pp. 371–386, 1991.
[11] J. C. Nedelec, "A new family of mixed finite elements in R^3," *Numerische Mathematik*, vol. 50, pp. 57–81, 1986.
[12] H. E. Bussey and L. A. Steinert, "Exact solution for a gyromagnetic sample and measurements on a ferrite," *IRE Trans. Microwave Theory Tech.*, vol. MTT-6, pp. 72–76, Jan. 1958.
[13] "Measuring methods for properties of gyromagnetic materials intended for application at microwave frequencies," IEC Standard Publication 556, Geneva, pp. 75–87, 1982.
[14] J. Krupka, "Measurement of all permeability tensor components and the effective linewidth of microwave ferrites using dielectric ring resonators," *IEEE Trans. Microwave Theory Tech.*, vol. 39, pp. 1148–1157, July 1991.
[15] J. Green and F. Sandy, "Microwave characterization of partially magnetized ferrites," *IEEE Trans. Microwave Theory Tech.*, vol. MTT-22, pp. 641–645, June 1974.
[16] E. Schloemann, "Microwave behavior of partially magnetized ferrites," *J. Appl. Phys.*, vol. 41, pp. 204–214, Jan. 1970.

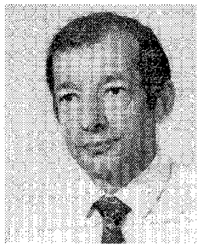

Jerzy Krupka was born in Cracow, Poland, in 1949. He received the M.Sc. (Hons.), Ph.D., and habilitation degrees from the Warsaw University of Technology in 1973, 1977, and 1989, respectively.

Since 1973, he has been with the Institute of Microelectronics and Optoelectronics, Warsaw University of Technology, where he is now an Associate Professor. His research deals mainly with numerical methods of electromagnetic field theory and measurements of the electric and magnetic properties of materials at microwave frequencies. He took part in several projects on these subjects in the US, France, Germany, and Australia.

Dr. Krupka is an Editorial Board Member of the IEEE TRANSACTIONS ON MICROWAVE THEORY AND TECHNIQUES.

Pierre Blondy was born in Limoges, France, on December 24, 1971. He received the Diplome d'Etudes Approfondies (D.E.A.) in microwave and optical communications from the University of Limoges in 1995.

Currently, he is working at Dassault Electronique, where he studied superconductors.

Dominique Cros was born in Millau, France, in June 1962. He received the Doctorat Thesis from the University of Limoges in 1990.

Currently, he is an Assistant Professor at the University of Limoges, working the Microwave and Optical Communications Research Institute. His main field of interest is the whispering gallery modes of dielectric resonators and their applications to millimeter-wavelength devices.

Pierre Guillon (SM'92) was born in May 1947. He received the Doctorat es Sciences degree from the University of Limoges, France, in 1978. From 1971 to 1980, he was with the Microwave and Optical Communications Laboratory, University of Limoges, where he studied dielectric resonators and their applications to millimeter-wave circuits.

From 1981 to 1985, he was a Professor of Electrical Engineering at the University of Poitiers, France. In 1985, he joined again the University of Limoges, where he is currently Professor and Head of Research Group in the area of microwave and millimeter-wave devices.

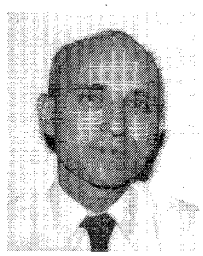

Richard G. Geyer was born in Lansing, MI. He received the B.Sc. (Honors) and Ph.D. degrees in 1966 and 1970 from Michigan State University and Colorado School of Mines, respectively.

Since 1970, he has been involved with measurements of the electronic and acoustic properties of materials and with numerical methods of electromagnetic and acoustic field theory. Since 1986, he has been at the National Institute of Standards and Technology within the Antenna and Electromagnetic Properties of Materials Metrology Group, where his research deals mainly with theory and applications of high-temperature superconductors, dielectric waveguides, dielectric resonators, microwave ferrites, and measurements of the electronic properties of materials at microwave frequencies.

Dr. Geyer is Chairman of the IEEE AP/MTT/GRS Joint Chapter of the Denver–Boulder Section. In 1972, he was given a best paper award for analytical work on transient electromagnetic scattering in an inhomogeneous penetrable halfspace.